Increasing the bandwidth of a SiGe HBT LNA with Minimum Impact on Noise Figure

Abadahigwa Bimana[†], *SMIEEE*, aba.bimana@ieee.org, and
Saurabh Sinha[†,††], *SMIEEE*, ssinha@ieee.org
†Carl & Emily Fuchs Institute for Microelectronics, Dept. of Electrical, Electronic and Computer Engineering, University of Pretoria, Pretoria, South Africa.
†† Faculty of Engineering and the Built Environment, University of Johannesburg, Johannesburg, South Africa.

***Abstract*—This paper introduces a matching technique for highly sensitive integrated broadband low-noise amplifiers. Noise matching is achieved by the paralleling of identical input transistors. Impedance matching, based on reducing the number of components to the absolute minimum, is done by using the base-collector capacitance as network element. Using a 0.13 μm silicon-germanium (SiGe) bipolar complementary metal oxide semiconductor process, simulation results indicate a maximum noise figure of 0.462 dB at room temperature and a return loss better than 10 dB from 300 MHz to 1.4 GHz. The technique demonstrates that SiGe heterojunction bipolar transistors can be used for cost-effective applications in radio astronomy.**

Key words: broadband amplifiers; heterojunction bipolar transistors; low-noise amplifiers; noise figure; radio astronomy.

1. INTRODUCTION

Advances in radio frequency (RF) integrated circuits have led to the integration of active and passive components on the same semiconductor substrate, departing from technologies from earlier generations that were initially based on discrete devices on printed circuit board and evolved to hybrid circuits, to multichip modules and to monolithic microwave integrated circuits. Despite the benefits of integration, such as high reliability, low cost, low power consumption and small size, the noise performance of RF integrated circuits is impaired by high losses caused by on-chip passive components, substrate losses and interconnection losses. A significant contribution to the noise figure (NF) of integrated low-noise amplifiers (LNA) is made by on-chip inductors, owing to their low quality factor.

In a typical LNA architecture, inductors and capacitors are required for input and output matching networks, with the highest degradation of noise performance being caused by the input matching network. While the number of passive components for noise and impedance matching can be low for narrowband topologies, this number may increase significantly for wideband

LNAs without resistive feedback. Resistive feedback increases the bandwidth but is avoided in sub-1 dB LNA designs, because of its additional thermal noise. For highly sensitive receivers, such as LNAs for radio astronomy, it is desired to reduce the number of passive components at the input to the absolute minimum, especially when the LNA is designed to operate at room temperature.

This paper presents a sub-1dB NF wideband LNA, in the frequency range of 0.3 GHz to 1.4 GHz, at room temperature. The LNA is based on 130 nm inductively degenerated common-emitter (IDCE) silicon-germanium heterojunction bipolar transistor (SiGe HBT) devices in a cascode configuration. Simultaneous noise and broadband power matching at the input are achieved by only one additional on-chip capacitor, whereas the capacitance of the reverse-biased base-emitter junction at the input transistor is used as circuit element. An output matching network based on a 4^{th} order Butterworth approximation, in conjunction with unconstrained non-linear optimization, is used to maximize the transfer of power between the output transistor and a 50 Ω load. The values of the elements of the matching network are derived from iterations performed by a MATLAB™ script resulting in optimum power transfer. The simulation with SpectreRF shows that maximum NF and gain of respectively 0.462 dB and 18 dB are achieved in the operating bandwidth.

This paper is structured as follows: Section 2 describes the noise and impedance matching proposed for a narrowband IDCE LNA. Section 3 investigates bandwidth extension techniques. A technique with minimum impact on NF is derived and presented in Section 4. The impact of the bandwidth extension technique on NF is analyzed in Section 5. Simulation results without output matching are presented in Section 6. The proposed output matching network is presented in Section 7. Simulation results of the output matched LNA are presented in Section 8 and the conclusions are found in Section 9.

2. NOISE AND IMPEDANCE MATCHING TECHNIQUES FOR LNAS

LNAs have relatively few components. However, their simplicity is misleading, as their design requires several trade-offs. Their performance metrics cannot be optimized simultaneously and complicated concessions are required between NF, bandwidth, gain, power consumption, supply voltage, dynamic range, linearity, stability and matching. In [1], a methodology for achieving

simultaneous low noise and impedance matching for SiGe HBT based LNAs for the Square Kilometre Array (SKA) is proposed. Owing to the large number of receivers required for the SKA [2], cost-effective LNAs are desired. SiGe HBT based LNAs are therefore low-cost alternatives compared to III-V technologies because of the high f_T and f_{MAX} of SiGe HBTs and their low parasitic resistances [3]. Low noise is obtained by optimal biasing of the input transistor, while noise and impedance matching is achieved through transistor sizing and the IDCE topology. The degenerated common-emitter topology is used in a cascode configuration, which enhances stability performance (through a high reverse isolation S_{12}) and facilitates input and output impedance matching. The cascode configuration, originating from vacuum tube amplifiers several decades ago, improves performance by decreasing the impact of the Miller's effect to the lower transistor. It also facilitates impedance matching in reducing the coupling between the output and the input. This configuration moreover limits antenna radiations possibly caused by the mixer stage.

The cascode configuration also has disadvantages, including a poor power supply rejection ratio, high output impedance and limited output voltage swing. In addition, the collector current densities of the top and bottom transistors are slightly different owing to the base current of the top transistor and to device mismatches. The LNA is represented in Figure 1 where Q_1 and Q_2 are equal in size. Linearity and gain can be improved when Q_2 is larger than Q_1, but possibly at the cost of a slight degradation of the NF. A small improvement of the NF can be achieved when Q_2 is slightly smaller than Q_1.

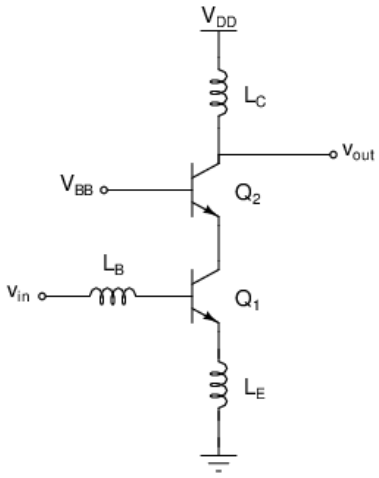

Figure 1 Inductively degenerated common-emitter cascode LNA.

Noise matching requirements for the circuit in Figure 1 can be analyzed by the classical two-port noise theory. The two-port noise theory, although underutilized in the design of LNAs since its presentation in 1960 [4], allows investigation of how the NF is related to the impedance of the source and the introduction of the concepts of minimum achievable noise factor F_{min}, noise resistance R_n, optimum source conductance G_{opt} and susceptance B_{opt}, with $G_{opt} + jB_{opt} = Y_{opt}$, Y_{opt} being the admittance of the source for which the noise factor is optimum. It can be shown that the noise factor F of a two-port network is given by [5]:

$$F = F_{\min} + \frac{R_n}{G_s}\left[\left(G_s - G_{opt}\right)^2 - \left(B_s - B_{opt}\right)^2\right] \qquad (1)$$

where G_s and B_s are respectively the conductance and the susceptance of the signal source.

The parameters F_{min}, R_n, G_{opt} and B_{opt} are known as the four noise parameters and provide, for resistive sources, the source resistance R_{sopt} for which the minimum NF is achieved, with $R_{sopt} = R_e\{1/G_{opt}\}$. The two-port noise theory allows determination of noise matching conditions, including R_n, the sensitivity of F to variations of the impedance of the source related to $1/Y_{opt}$. Equation (1) shows that, in order to achieve a low F, F_{min} and R_n are required to be low and Y_s must be equal or close to Y_{opt}, with $Y_s = G_s + jB_s$.

2.1 Noise Matching

The performance of receivers is affected by undesired components such as hum, interference and distortion. Moreover, supply sources produce noise and can introduce external noise in the signal path [6]. However, such noise is extrinsic to receivers and, contrary to intrinsic noise, can generally be suppressed. Intrinsic noise in RF amplifiers is random and mainly due to active components, matching networks and the direct current (DC) biasing circuitry. Noise in active components and in biasing circuitry is of thermal, shot, flicker, avalanche and generation-recombination types, while in passive matching networks, the noise is mainly thermal [5]. In active devices, electronic noise is related to their specifications, to temperature, to the bias current and to the operating frequency. For SiGe HBTs, intrinsic noise is closely related to parasitic resistances such as base and emitter resistances r_b and r_e, the unity gain frequency f_T and the current gain β_o. It is shown in [7] that, for the common-emitter configuration, F_{min} for SiGe HBTs is given by:

$$F_{\min} = 1 + \frac{n}{\beta_o} + \sqrt{\frac{qI_C}{2kT}(r_b + r_e)\left(\frac{f^2}{f_T^2} + \frac{1}{\beta_o}\right) + \frac{n^2}{\beta_o}} \qquad (2)$$

where I_c is the collector current, q is the electron charge, k is the Boltzmann constant, T the absolute temperature, n the collector ideality factor and f the operating frequency.

It can also be shown that F_{min} reaches a minimum for $I_c = I_{copt}$, corresponding to the emitter current density J_{copt}. Furthermore, F_{min} is invariant to I_c as long as J_{copt} is constant. Hence, for a given technology process, the same minimum value of F_{min} is achieved by transistors of different emitter length (l_e) and width (w_e) when J_{copt} is constant.

The noise resistance R_n and the source resistance for minimum noise R_{sopt} are given by the following equations for the common emitter SiGe HBT [7]:

$$R_n \approx \frac{n^2 V_T}{2J_c w_e l_e} + (r_{bl} + r_{el})\frac{1}{l_e} \qquad (3)$$

$$R_{sopt} \approx \frac{R_n f_T}{f} \frac{\sqrt{\frac{I_C}{2V_T}(r_b + r_e)(1 + \frac{f_T^2}{\beta_o f^2}) + \frac{n^2 f_T^2}{4\beta_o f^2}}}{\frac{I_C}{2V_T}(r_b + r_e)(1 + \frac{f_T^2}{\beta_o f^2}) + \frac{n^2}{4}\left(1 + \frac{f_T^2}{4\beta_o f^2}\right)} \qquad (4)$$

where $r_{bl} = r_b l_e$ and $r_{el} = r_e l_e$ are technology constants, $n = 1$ and J_c is the emitter current density.

If I_c is replaced by $J_c w_e l_e$, (4) is rewritten as:

$$R_{sopt} \approx \frac{R_n f_T}{f} \frac{\sqrt{\frac{J_C w_e}{2V_T}(r_b l_e + r_e l_e)(1 + \frac{f_T^2}{\beta_o f^2}) + \frac{n^2 f_T^2}{4\beta_o f^2}}}{\frac{J_C w_e}{2V_T}(r_b l_e + r_e l_e)(1 + \frac{f_T^2}{\beta_o f^2}) + \frac{n^2}{4}\left(1 + \frac{f_T^2}{4\beta_o f^2}\right)}. \qquad (5)$$

The second factor of (5) is not related to l_e for a given emitter width, technology process, current density and operating frequency. Therefore, R_{sopt} is proportional to $1/l_e$ and noise matching can be achieved by varying the length of the emitter. For submicron technologies, R_{sopt} can be much higher than the source resistance, which is typically 50 Ω at microwaves and for devices of

maximum size for the manufacturing technology. In such a case, several transistors can be connected in parallel. It is shown in [8] that the NF is invariant to the paralleling of identical transistors and that R_{opt} is inversely proportional to the number of transistors in parallel.

2.2 Impedance Matching

The input impedance of the amplifier in Figure 1 can be expressed by (6), for frequencies that are much lower than f_T, for which the impact of the Miller effect on the input transistor can be neglected.

$$Z_{in} = r_b + \frac{I_c q}{kTC_\pi} L_E + j\omega\left(L_B + L_E\right) - \frac{j}{\omega C_\pi} \cong r_b + \omega_T L_E + j\omega\left(L_B + L_E\right) - \frac{j}{\omega C_\pi} \quad (6)$$

with $\frac{I_c q}{kTC_\pi} = \frac{g_m}{C_\pi} \cong \omega_T$ where C_π is the base-emitter capacitance, g_m the transconductance, ω the angular frequency, and $\omega_T = 2\pi f_T$.

From (6), it is found that the real part of Z_{in} is independent of frequency and is related to the emitter inductor L_E, to the transconductance g_m and to the base-emitter capacitance C_π. The impedance of the emitter inductor L_E is seen as a real resistance when viewed from the input. Hence, this inductor can be used to match the real part of the input impedance to the resistance of the source. The input impedance also has a capacitive reactance, due to the base-emitter capacitance C_π, which must be cancelled by an inductive reactance for resistive sources. The capacitive reactive component is cancelled by L_E and by the inductor L_B in the base circuit, an inductor that is sized to resonate with L_E and C_π at the operating frequency. Impedance matching is achieved in a narrow frequency band whose bandwidth is determined by the quality factor Q_{in} at the input. Narrow bandwidth refers to a bandwidth of less than 20% of the center frequency [1].

In summary, minimum noise is achieved by the biasing of the input transistor at I_{copt}, while noise and power matching are achieved when the source resistance R_s, when R_{sopt}, L_B and L_E are related by the equations [9]:

$$R_s \cong r_b + \omega_T L_E \quad (7)$$

$$L_B \cong \frac{1}{\omega^2 C_\pi} - L_E \quad (8)$$

$$R_s \cong R_{sopt} \quad (9)$$

$$\omega L_B = X_{opt} - \omega L_E \quad (10)$$

where X_{opt} is the imaginary part of $1/Y_{opt}$.

3. BANDWIDTH EXTENSION FOR LNAs

The noise performance of an LNA is strongly related to the noise caused by the input matching network, whereas the impact of the output matching network on noise performance is small and can be negligible, as indicated by Friis's formula [10]. The desired input impedance can be attained by noiseless or noisy input matching networks or by the use of feedback networks. For narrowband applications, simple matching can be achieved by the use of L, T or Π networks.

Bandwidth is easily increased by a shunt resistance at the input or by resistive feedback. However, the shunt and feedback resistances increase the NF and reduce the gain. Typically, the NF increases by more than 6 dB in the case of resistive shunt while the impairment is smaller for resistive feedback, the resistance used in the resistive feedback generally being high. It may then appear that wideband matching for ultra-low noise amplifiers can only be achieved by complex matching networks and by configurations such as balanced amplifiers, distributed amplifiers and transmission lines. The power consumption of these configurations is high and they entail large areas of the chip. In addition, balanced amplifiers demand large quadrature couplers that increase losses [11]; their noise performance is not better than 3 dB [12]. Bandwidth increase can also be attained by impedance transformers, by emitter degeneration with resistive and capacitive loading [13] and by input matching networks such as ladder filters [14].

It has been shown that traditional techniques used for bandwidth expansion require additional components at the input, components that impair the noise performance of the LNA. Such techniques include the use of an impedance transformer and of various types of broadband matching networks. As any additional component in the input network affects the NF, it is desirable to reduce the number of matching components to the strict minimum. In addition, to

limit the impact of bandwidth increase to the NF, resistive components cannot be used in the signal path, through matching or feedback networks.

4. BANDWIDTH EXTENSION TECHNIQUE

The input matching of the broadband common-source inductively degenerated LNA in [16] is investigated in [13]. It is found that, for low frequencies, input matching is achieved by the capacitive feedback from the capacitive load in series with a resistor through the gate-drain capacitance. For high frequencies, matching is obtained owing to the inductive feedback in the source circuit. The LNA requires few components at its input and uses the intrinsic gate-drain capacitance coupled to an external capacitor between the drain of the input transistor and the source of the cascode transistor to increase the matching bandwidth. The design strategy constitutes using unfavorable circuit characteristics such as parasitics as circuit elements. This is well paraphrased by Thomas Lee in the preface of [15]: “To no small degree, an important lesson in RF and microwave design is that there are always irreducible parasitics. Rather than conceding defeat, one must exploit them as circuit elements.” A detailed analysis of the bandwidth expansion of a SiGe HBT based LNA with minimal impact on noise performance is provided in this section.

A simplified small-signal model of a cascode amplifier is shown in Figure 2, where the parasitic base and emitter resistances are neglected and the input impedance of the cascode transistor is Z_L. The input impedance has been estimated in (6), where the base-collector capacitance C_μ = C_{bc} has been neglected. Neglecting the base resistance as well, the input impedance at the base is given by the expression:

$$Z_{in} \cong \omega_T L_E + j\omega\left(L_E\right) - \frac{j}{\omega C_{be}}. \qquad (11)$$

Taking into account the effect of the base-collector capacitance, the input impedance is equal to $Z_{in} \| \frac{1}{Y_b}$ where Y_b is the admittance seen at the base, after the input capacitor C_{be} as shown in Figure 2.

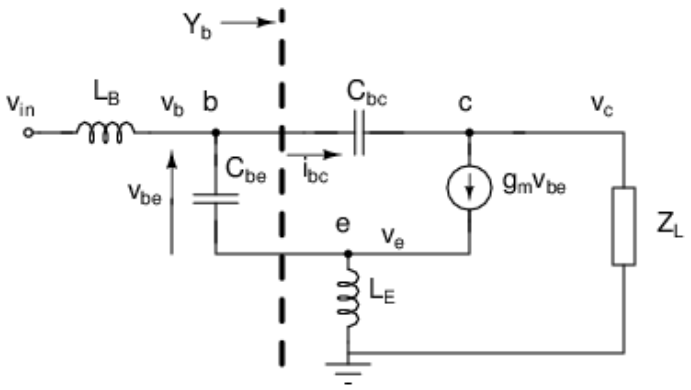

Figure 2 Simplified small-signal model of the IDCE cascode amplifier.

The admittance Y_b is calculated by dividing the current i_{bc} by the voltage v_b and it can be shown that Y_b is given by:

$$Y_b = j\omega C_\mu + \frac{j\omega C_\mu g_m Z_L}{1 + j\omega L_E g_m}. \qquad (12)$$

Hence, the admittance Y_b is given by $Y_b = Y_1 || Y_2$ with $Y_1 = j\omega C_\mu$ and $Y_2 = \frac{j\omega C_\mu g_m Z_L}{1 + j\omega L_E g_m}$.

Therefore Y_b is the result of a capacitor C_μ in parallel with the impedance $Z_2 = 1/Y_2$.

The impedance Z_2 is rewritten as:

$$Z_2 = \frac{(1 + j\omega L_E g_m) Y_L}{j\omega C_\mu g_m} \qquad (13)$$

where $Y_L = 1/Z_L$.

A capacitor of value C_L is added between the collector of the input and the emitter of the cascode transistor. Z_L is then seen as r_o in parallel with C_L in series with $1/g_m$, $1/g_m$ being the input resistance of the common-base cascode transistor. The transconductances of both the input and cascode transistors are identical. The impedance Z_L is represented in Figure 3.

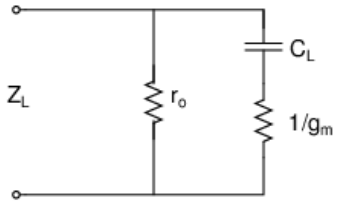

Figure 3 Impedance at the output of the input transistor.

The expression of Z_L is given by:

$$Y_L = \frac{1}{r_o} + \frac{j\omega g_m C_L}{g_m + j\omega C_L}. \qquad (14)$$

In replacing Y_L by its expression in (14), (13) becomes:

$$Z_2 = \frac{1}{j\omega C_\mu g_m r_o} + \frac{L_E}{C_\mu r_o} + \frac{(1 + g_m j\omega L_E)}{g_m j\omega C_\mu} \frac{j\omega C_L g_m}{(g_m + j\omega C_L)}. \qquad (15)$$

Equation (15) shows that Z_2 is formed by a capacitor of value $C_\mu g_m r_o$, a resistance of value $\frac{L_E}{C_\mu r_o}$ and an impedance Z_3 equal to the last term of (15), all in series.

The impedance Z_3 is given by:

$$Z_3 = \frac{C_L}{C_\mu (g_m + j\omega C_L)} + \frac{L_E j\omega C_L g_m}{C_\mu (g_m + j\omega C_L)}. \qquad (16)$$

The impedance Z_3 is equal to the sum of Z_4 and Z_5, given by the relations:

$$Z_4 = \frac{C_L}{C_\mu (g_m + j\omega C_L)} \qquad (17)$$

$$Z_5 = \frac{L_E j\omega C_L g_m}{C_\mu (g_m + j\omega C_L)}. \qquad (18)$$

The impedance Z_4 is equivalent to a resistor of value $\frac{C_L}{C_\mu g_m}$ in parallel of a capacitor of value C_μ. The impedance Z_5 is equivalent to a resistor of value $\frac{L_E g_m}{C_\mu}$ in parallel with an inductance of value $\frac{L_E C_L}{C_\mu}$.

Combining Z_{in} and the successive impedance transformations of Z_L, the input impedance of the cascode amplifier is represented in Figure 4.

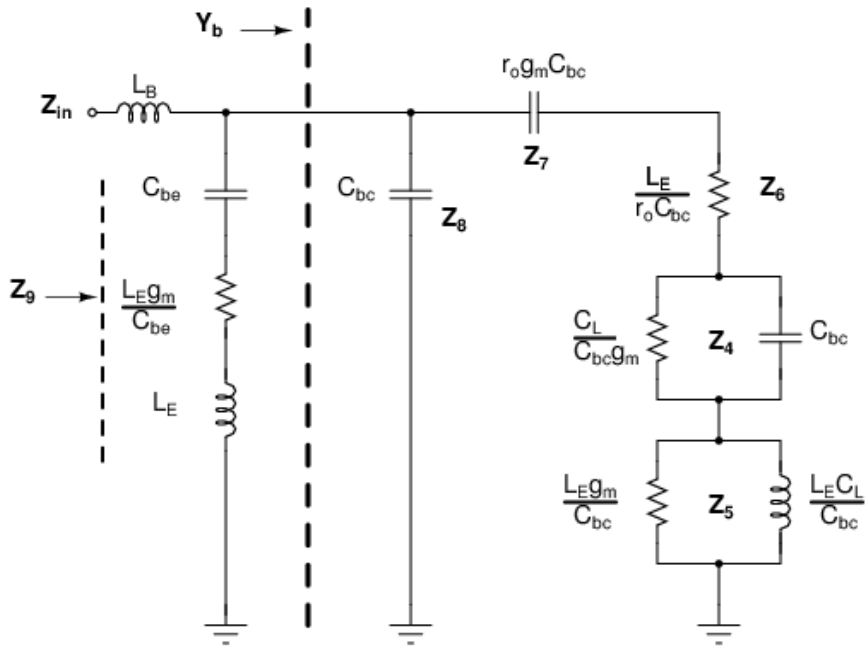

Figure 4 Input impedance of the modifier cascode amplifier.

The circuit in Figure 4 is a double-tuned resonant circuit with the inductance L_B in series with the impedance Z_9, being the first RLC tuned circuit. The resonant frequency f_1 of this circuit is given by:

$$f_1 = \frac{1}{2\pi\sqrt{(L_B + L_E)C_{be}}}. \qquad (19)$$

The order of magnitude of passive components of Figure 4 is evaluated from the typical parameters of a six-finger SiGe HBT. The transistor is biased at a base voltage of 0.867 V and

the area of the transistor is $0.12 \times 6 \times 1$ μm^2. For an operating frequency of 1 GHz, it can be shown that Z_4 is mainly resistive and that Z_5 is inductive. Hence, Z_7, Z_4 and Z_5 form the second tuned RLC circuit. The frequency f_2 of this tuned circuit can be approximated by:

$$f_2 = \frac{1}{2\pi\sqrt{r_o g_m L_E C_L}} \quad . \tag{20}$$

Resonance at f_2 is due to capacitive feedback and f_2 is lower than f_1, the values of the capacitance of Z_7 and of the inductance in Z_5 being higher than C_π and $L_B + L_E$. Owing to an adequate determination of the frequencies f_1 and f_2, the combined impedance of the coupled tuned circuits can achieve an input reflection coefficient S_{11} that is less than -10 dB in a wide band.

5. IMPACT ON NF

The second stage of the cascode amplifier being coupled to the first stage through the capacitor C_L, the question of the impact of this coupling on the NF arises. Assuming that the gain of the input stage is high, the contribution of the second stage (Q_2) to the NF is neglected. The bandwidth-enhanced cascode LNA is represented in Figure 5 as a cascade of two two-port networks formed by Q_1, the input transistor, and C_L.

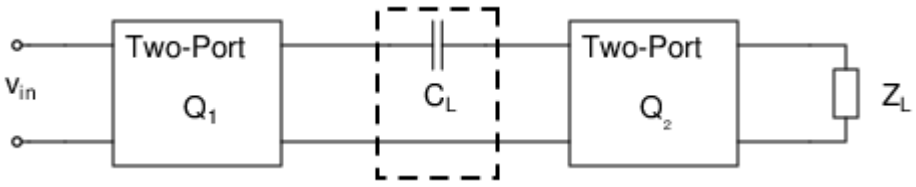

Figure 5 Bandwidth-enhanced cascode LNA.

The NF of the two-port networks in Figure 5 is given by:

$$F = 1 + \frac{Z^+ C_A Z}{2kT\,\mathrm{Re}\{Z_S\}} \tag{21}$$

where C_A is the noise correlation matrix of the cascaded network resulting from Q_1 and C_L, Z_s is the impedance of the source, Z^+ is the Hermitian conjugate of Z with $Z = \begin{bmatrix} 1 \\ Z_s^* \end{bmatrix}$. The noise correlation matrix C_A is expressed as:

$$C_A = A_1 C_{A2} A_1^+ + C_{A1} \qquad (22)$$

where A_1 is the transmission matrix of the input stage and C_{A1} is its noise correlation matrix. C_{A2} is the noise correlation matrix of the two-port network formed by C_L.

The noise correlation matrix C_{A2} is nil, as its diagonal terms are real values that represent the power spectrum of each noise source and the off-diagonal terms represent their cross-power spectra; these terms are nil for a noiseless network. The noise correlation matrix of the input stage is given by:

$$C_{A1} = 2kT \begin{bmatrix} R_n & \left[\frac{F_{\min} - 1}{2} - R_n Y_{sopt}^* \right] \\ \left[\frac{F_{\min} - 1}{2} - R_n Y_{sopt} \right] & R_n \left| Y_{sopt} \right|^2 \end{bmatrix}. \qquad (23)$$

It is then concluded that C_A is not related to C_L, hence C_L does not impair the noise factor of the LNA.

6. SIMULATION RESULTS

SiGe HBTs of maximum size ($0.12 \times 18\ \mu m^2$) from the 130 nm IBM BiCMOS8HP process are used for the cascode configuration. F_{min} and R_{opt} for the cascode LNA are determined by simulation with SpectreRF. Noise matching is done at the high end of the frequency band since, F_{min} being an increasing function of frequency, the minimum achievable noise is better than F_{min} in the bandwidth of the LNA. It is found that F_{min} = 0.337 dB and that the base bias voltage V_B required for minimum NF is 0.7705 V at 1.4 GHz. The plot of F_{min} as a function of V_B is shown in Figure 6.

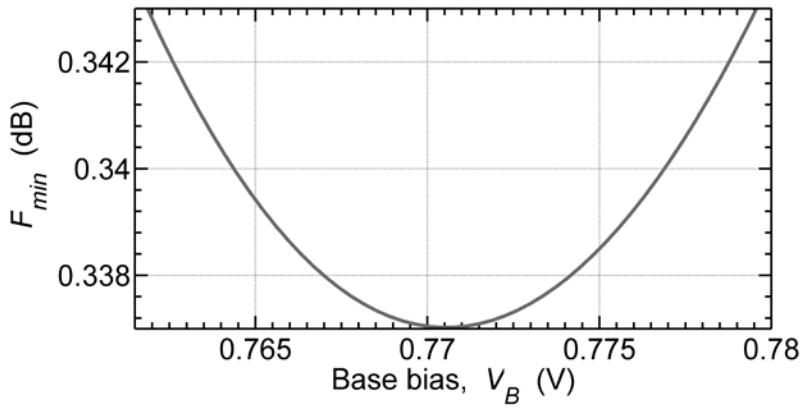

Figure 6 Optimum base bias voltage for the cascode amplifier.

A parametric plot of R_{opt} as a function of frequency allows one to determine that 14 parallel transistors are required for noise matching at 1.4 GHz. R_{opt} is chosen to be slightly higher than 50 Ω because of the parasitic resistance of the base inductor L_B. The impact of transistor paralleling on F_{min} is negligible, F_{min} is unchanged when 14 transistors are connected in parallel at the input and at the output. The base inductor is approximated by matching the reactive part X_{opt} of the noise impedance to L_B. Hence, at 1.4 GHz, NF = F_{min}. The emitter inductor is calculated from (7) and then fine-tuned by simulation of $S_{11,}$ as shown in Figure 7.

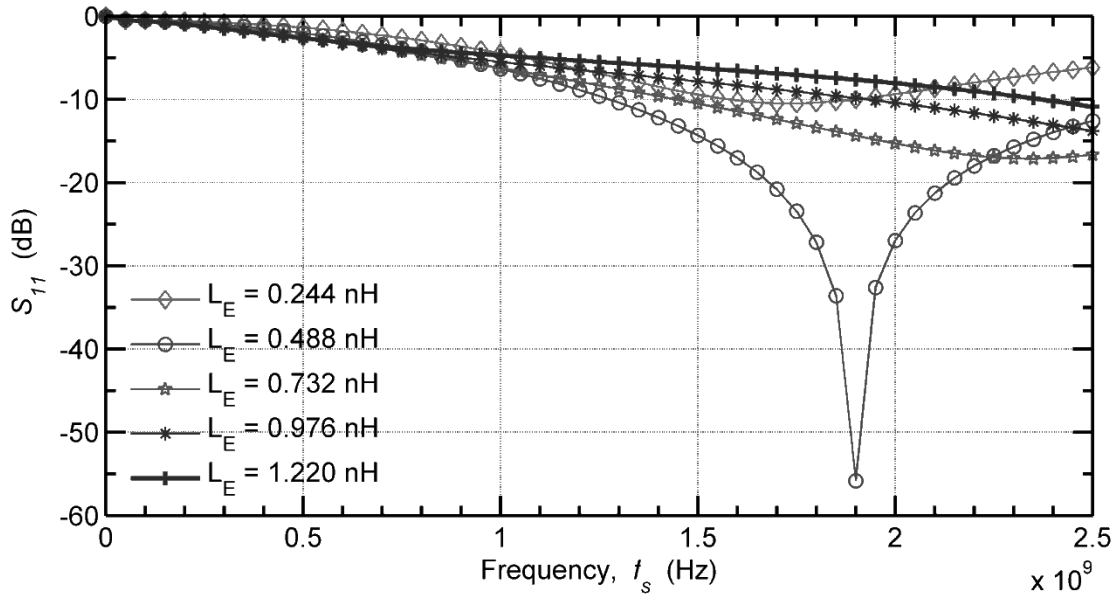

Figure 7 S_{11} versus frequency and L_E.

As L_B has been determined on the basis of noise matching only, the addition of L_E cancels the noise matching at 1.4 GHz and the relation between L_B and L_E is determined by (10). Therefore, the imaginary part of Z_{in} is not nil at 1.4 GHz. A new value of L_B is determined by a parametric simulation of NF as a function of frequency and of L_B. The resonant frequency of the input matching circuit is found by simulation of S_{11} as a function of frequency. It is found that S_{11} is minimal at 1.89 GHz, a frequency higher than 1.4 GHz at which noise matching has been performed. Therefore, noise is matched at 1.4 GHz while power is matched at 1.89 GHz, which improves bandwidth extension. The latter frequency corresponds to f_1, as predicted in Section 4 and given by (19).

Narrowband matching being achieved, a capacitor C_L is introduced between the collector of the input transistor and the emitter of the cascode transistor. The value of C_L is found by seeking a flat response for S_{11} in the operating bandwidth.

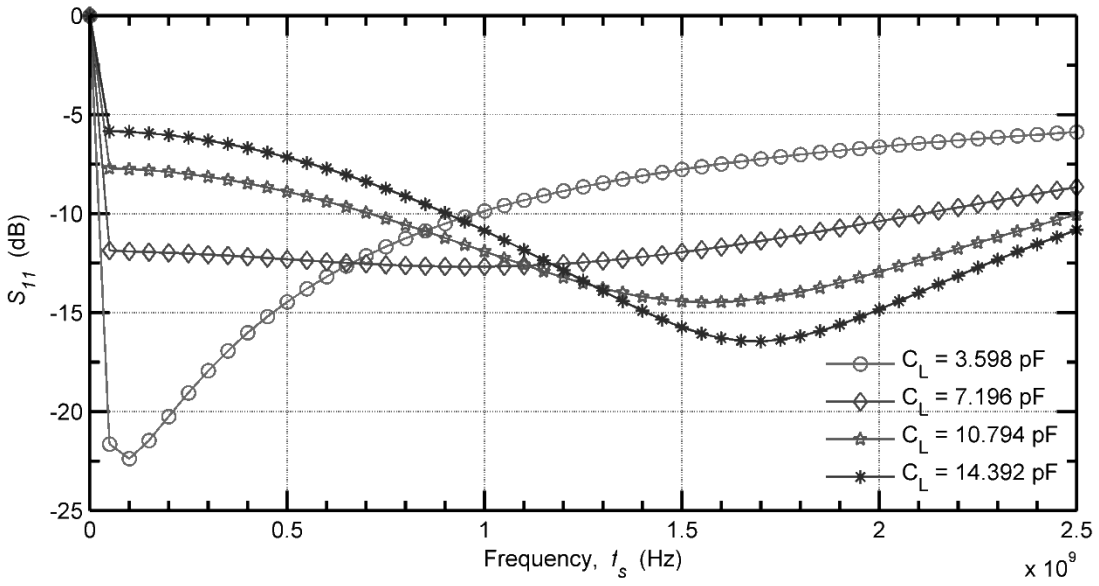

Figure 8 Determination of C_L by parametric simulation of S_{11} versus frequency.

For C_L equal to 7.196 pF, S_{11} is near-flat and is less than –10 dB in a wide input frequency band of the LNA, from 300 MHz to 1.4 GHz. For low values of C_L, the lower resonant frequency f_2 is dominant in S_{11} response. For high values of C_L, S_{11} tends to its minimum value, as shown in Figure 8, and the frequency f_1 tends to 1.89 GHz.

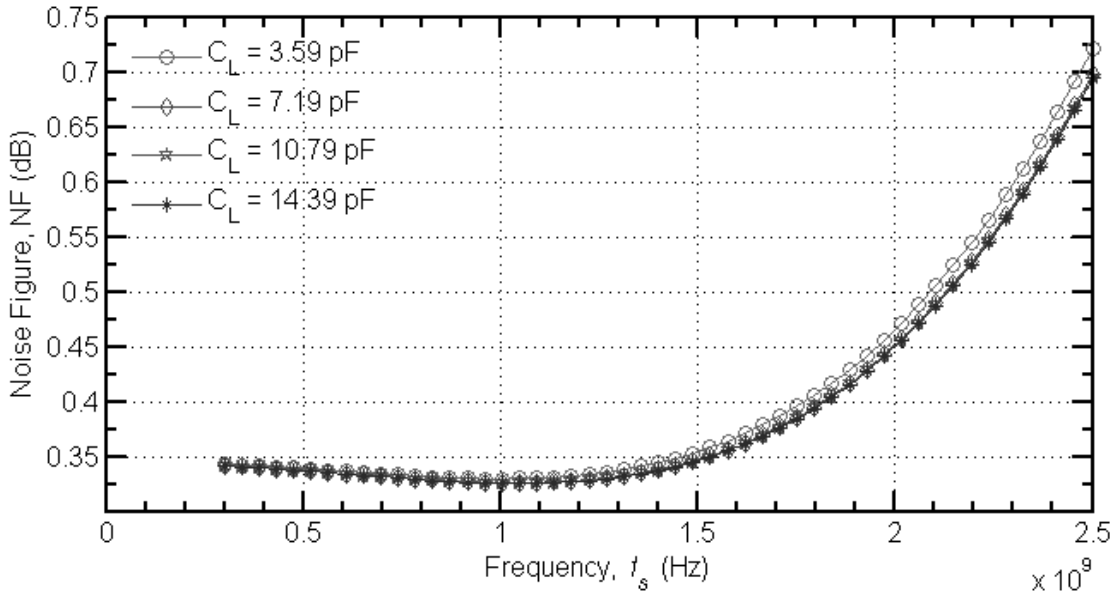

Figure 9 NF versus frequency and $C_{L.}$.

The plot of the NF shows in Figure 9 that the effect of C_L on the NF is very small and that the NF varies slightly in the LNA bandwidth. At 1.4 GHz, the NF increases by about 0.002 dB. However, for low values of C_L, the NF increases significantly.

7. OUTPUT MATCHING

The output impedance of the LNA is large, compared to the 50 Ω of the load. In order to reduce NF impairments due to the matching network, a network with only reactive components is desired. However, a tentative preliminary design of the matching network done with the Smith chart shows that the trace of the reflection coefficient remains on the outer boundary of the chart; for the trace to move on circles of constant resistance on the Z and Y circles of the chart, a resistance R_L is required at the output of the LNA, as shown in Figure 10. Although inductive peaking [17] is also a possible solution, it increases the operating voltage and significantly impairs the noise performance.

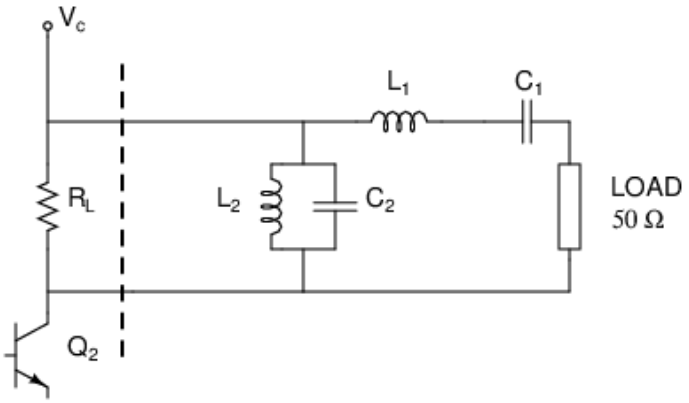

Figure 10 Output matching network.

A trade-off is required between NF and output matching: both the noise performance and the gain decrease with R_L but the matching is impaired. For R_L=90 ohms, it is found that broadband matching can be achieved by the network represented in Figure 10, which may represent a 4th order Butterworth or Chebyshev band-pass approximation, depending on the values of passive components. Although a passband filter can considerably reduce undesired signals, it does not maximize the transfer of power from its input to the output, unless the impedance of the input signal source is equal to the complex conjugate of the input impedance of the filter and the complex conjugate of the load impedance is equal to the output impedance of the filter. A MATLAB™ script is used to minimize the reflection of power resulting from a 4th order filter based on a Butterworth approximation within the operating bandwidth. The script is based on the brute force technique that uses a computer-aided design tool to fine-tune the elements of a matching network based on a predetermined topology.

8. FINAL LNA CIRCUIT

The LNA circuit is represented in Figure 11, where the bias network is not shown. The base inductor L_B and the choke are off-chip; all other components are on-chip. The size of SiGe HBTs used is 0.120 μm × 18 μm with a multiplicity factor of 14; the supply voltage is 2.2 V.

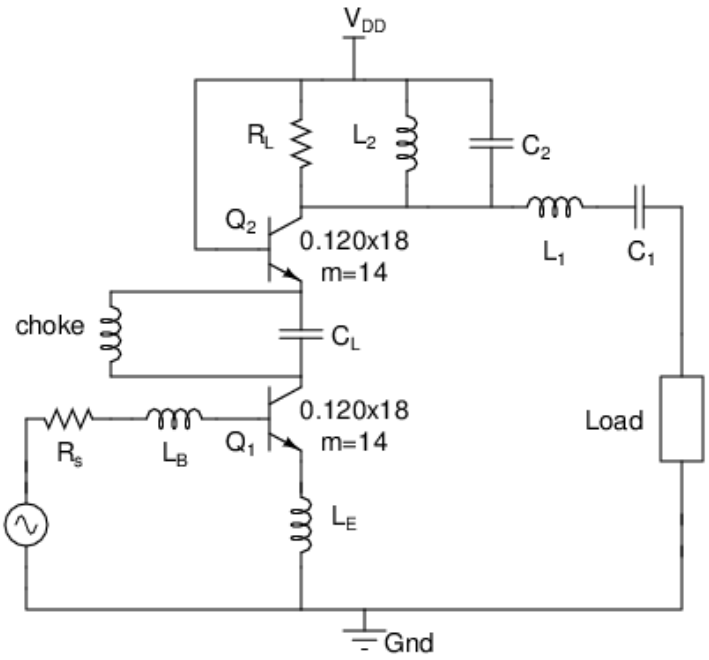

Figure 11 LNA circuit.

The resistance of the source is R_s, both R_s and the resistance of the load are equal to 50 Ω. The plots of the NF, S_{11} and S_{22} are shown in Figure 12. The gain G_A, S_{21} and S_{12} are plotted in Figure 13 and Figure 14, respectively. The NF is less than 0.462 dB, S_{11} and S_{22} are less than –10 dB from 300 MHz to 1.4 GHz. All components are from the 130 nm IBM BiCMOS8HP process and correspond to eight layers of metal, except for the base inductor L_B and the choke, which are external.

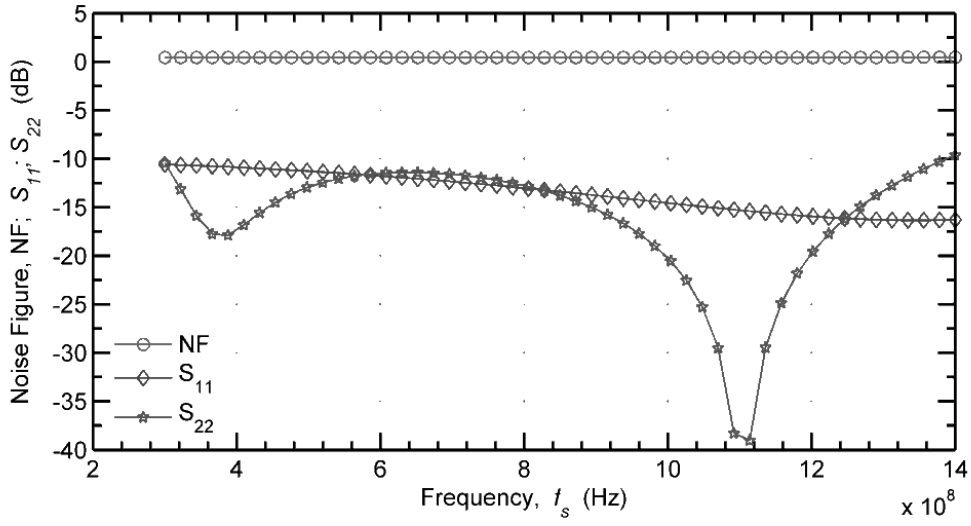

Figure 12 NF, S_{11} and S_{22} simulation by SpectreRF.

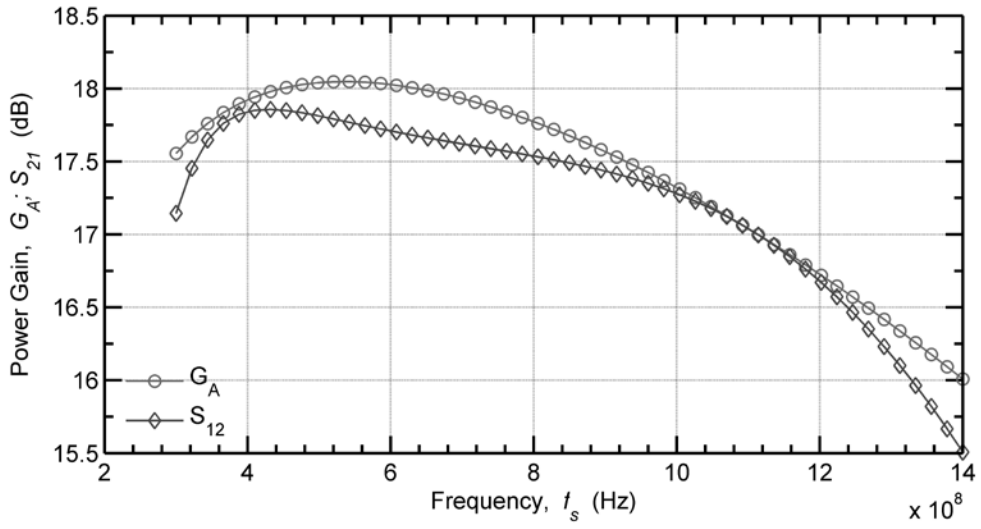

Figure 13 G_A and S_{21} frequency response

.

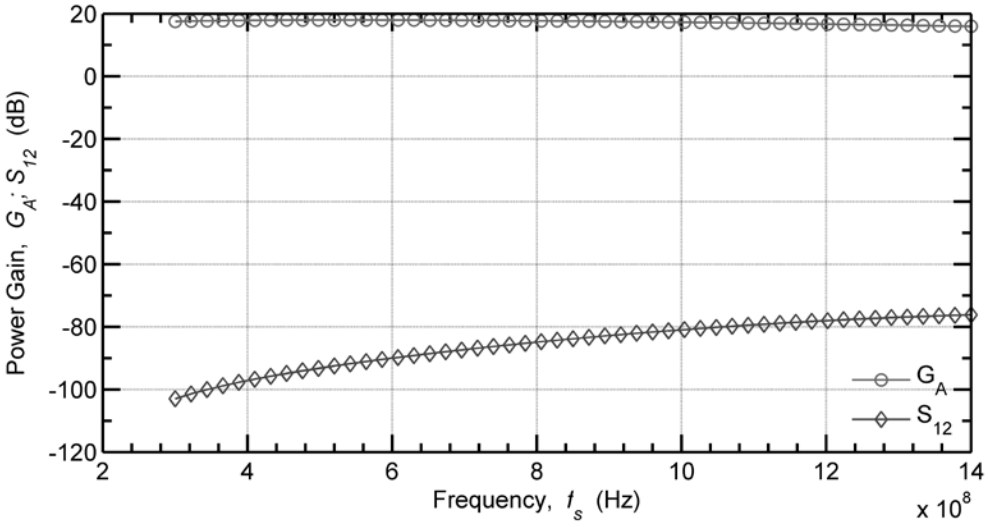

Figure 14 S_{12} frequency response.

The comparison between performance metrics of similar LNAs for radio astronomy and the impact of process, temperature, integration and bandwidth on performance is shown in Table 1.

Table 1 Performance comparison with similar reported LNA designs.

Property	**[18]**	**[19]**	**[20]**	**[21]**	**[22]**	**This work (simulation)**
Technology (μm)	0.090 CMOS	0.130 IBM BiCMOS8HP	MMIC 0.130 IBM BiCMOS8HP	1, InGaAs/InAlAs/ Inp HEMT	MIC Discrete pHEMT	0.130 IBM BiCMOS8HP
Frequency (GHz)	0.7 -1.4	0.7-3	0.1-5	1-3	0.02-1	0.3-1.4
NF (dB)	0.35	< 0.1	1	0.4	0.55	0.46
S_{11} (dB)	< -11	< 0	-8.4 @ 1.4 GHz	8.2 @ 1.4 GHz	< -4.5	< -10
S_{21} (dB)	20.5-16.3	32.8	28.3 @ 1.4 GHz	-16.5 @ 1.4 GHz	> 36	17.8 max
S_{22} (dB)	< -8	< -12	-16 @ 1.4 GHz	-12.5	< -10	< -10
Gain (dB)	17	28	27	30	30	18
Supply (V)	1	0.6	-	1.8	1	2.2
Supply (mA)	45	7.1	-	47	25	6
Source resistance (Ω)	50	50	50	50	50	50
Single-Ended/Balanced	S.E.	S.E.	S.E.	S.E.	S.E.	S.E.
Temperature (K)	Room	Cryogenic (15)	Room	Room	Room	Room
Area (mm^2)	0.81	-	-	Results from simulation	-	1.4
External coils	2	3	5 bond wires	0	-	2
Publication year	2007	2007	2009	2010	2014	2016

9. CONCLUSION

A novel bandwidth expansion technique with minimum impact on NF has been proposed for integrated narrowband cascode SiGe HBT LNAs. This technique achieves wideband impedance matching at the input of the LNA by reducing to the absolute minimum the number of passive components and by using the capacitance of the reverse biased base-collector junction of the input transistor as network element. Input impedance matching is based on the coupling of two resonant circuits, resulting in the sharing of the energy of each tuned circuit by the other. Noise

matching is done by varying the length of the emitter of transistors or by shunting several identical transistors.

The technique is applied to a sub-1 dB narrowband SiGe HBT LNA. It can be shown that the bandwidth of the narrowband LNA can be expanded more than five times, from 177 MHz to more than 1.1 GHz, for applications in radio astronomy for the SKA. The impact on the NF is noticeably small and simulation by SpectreRF shows that the NF increases from 0.337 dB to 0.462 dB at room temperature. The maximum gain of the LNA is close to 18 dB, S_{11} and S_{22} are less than -10 dB in the bandwidth of the LNA.

Simulation has shown that the increase in the NF is mainly due to losses in the inductors of the output matching network. The base inductor L_B and the choke are off-chip, the emitter inductor L_E and inductors of the output matching network are on-chip. The noise performance of the LNA can be improved when inductors with a high quality factor are used.

REFERENCES

[1] A. Bimana and S. Sinha, “Impact of SiGe parameters to the performance of LNAs for highly sensitive SKA receivers." In *Radioelektronika (RADIOELEKTRONIKA), 2013* 23rd *International Conference*, pp. 50-54. IEEE, 2013.

[2] D.M.P. Smith, L. Bakker, R.H. Witvers, B.E.M. Woestenburg and K.D. Palmer, “Low noise amplifier for radio astronomy,” *Int J.Microw. Wirel. Technol.*, vol. 5, no. 04, pp. 453-461, August 2013.

[3] E. Ojefors, F. Pourchon, P. Chevalier and U.R. Pfeiffer, “A 160-GHz low-noise downconversion receiver front-end in a SiGe HBT technology,” *Int J.Microw. Wirel. Technol.*, vol. 3 no. 03, pp. 347-353, June 2011.

[4] H.A. Haus, W.R. Atkinson, G.M. Branch, W.B. Davenport, W.H. Fonger, W.A. Harris, S.W. Harrison, W.W. McLeod, E.K. Stodola and T.E. Talpey, “Representation of noise in linear twoports,” *Proc. IRE*, vol. 48, no. 1, pp. 69-74, 1960.

[5] G. Vasilescu, *Electronic Noise and Interfering Signals: Principles and Applications.* Springer-Verlag, Heidelberg, Germany, 2005.

[6] E.H. Nordholdt, *Design of High-Performance Negative Feedback Amplifiers*. Elsevier Scientific, Amsterdam, 1983.

[7] S.P. Voinigescu, M.C. Maliepaard, J.L. Showell, G.E. Babcock, D. Marchesan, M. Schroter, P. Schvan and D. Harame, "A scalable high-frequency noise model for bipolar transistors with application to optimal transistor sizing for low-noise amplifier design," *IEEE J. Solid-State Circuits*, vol. 32, no. 9, pp. 1430–1438, 1997.

[8] L.N. Tran, "Caractérisation d'interconnexions et d'inductances en technologie BiCMOS. Application à l'amplification faible bruit," Ph.D. dissertation, University of Cergy-Pontoise, Paris, France, May 2009.

[9] S. Voinigescu, *High-Frequency Integrated Circuits*. Cambridge Univ. Press, New York, 2013.

[10] H.T. Friis, "Noise figure of radio receivers," *Proc. IRE*, vol. 32, no. 7, pp. 419-422, July 1944.

[11] D.M.P. Smith and B.E.M. Woestenburg, "Technique for reduction of noise resistance in a balanced low-noise amplifier for beam-steering applications," *Int J.Microw. Wirel. Technol.*, vol. 5, no. 05, pp. 561-565, October 2013.

[12] A. Bevilacqua and A.M. Niknejad, "An ultrawideband CMOS low noise amplifier for 3.1–10.6 GHz wireless receivers," *IEEE J. Solid-State Circuits*, vol. 39, no. 12, pp. 2259–2268, December 2004.

[13] R. Hu and M.S.C. Yang, "Investigation of different input-matching mechanisms used in wide-band LNA design," *Int. J. Infrared Millimeter Waves*, vol. 26, no. 2, pp. 221–245, February 2005.

[14] A.M. Niknejad, *Electromagnetics for High-Speed Analog and Digital Communication Circuits*. Cambridge Univ. Press, 2007.

[15] T. Lee, *Planar Microwave Engineering: A Practical Guide to Theory, Measurement and Circuits*. Cambridge Univ. Press, 2004.

[16] N. Wadefalk, A. Mellberg, I. Angelov, M. Barsky, S. Bui, E. Choumas, R. Grundbacher, E. Kollberg, R. Lai, N. Rorsman, P. Starski, D. Stenarson, J. Streit and H. Zirath, "Cryogenic wide-band ultra-low-noise IF amplifiers operating at ultra-low DC power," *IEEE Trans. Microwave Theory Tech.*, vol. 51, no. 6, pp. 1705–1711, June 2003.

[17] M.T. Hsu, S.Y. Hsu and Y.H. Lin, "Low-power CMOS LNA based on dual resistive-feedback structure with peaking inductor for wideband application," *Int J.Microw. Wirel. Technol*, vol. 5 no. 01, pp. 65-70, February 2013.

[18] L. Belostotski and W. Haslett, "Wide band room temperature 0.35-dB noise figure LNA in 90-nm bulk CMOS," in *Proc. IEEE Radio Wireless Symp*., Long Beach, CA, Jan. 7-11, 2007, pp. 221-224.

[19] S. Weinreb, J.C. Bardin and H. Mani, "Design of cryogenic SiGe low-noise amplifiers," *IEEE Trans. Microwave Theory Tech.*, vol. 55, pp. 2306-2312, November 2007.

[20] S. Weinreb, J.C. Bardin and H. Mani, "A 0.15-5 GHz cryogenic SiGe MMIC LNA," *IEEE Microwave and Wireless Comp. Lett*., vol. 19, no. 6, pp. 407-409, June 2009.

[21] Z. Hamaizia, N. Sengouga, M. Missous and M.C.E. Yagoub, "A 0.4 dB noise figure wideband low-noise amplifier using a novel InGAs/InAlAs/InP device," *Materials Science in Semiconductor Processing*, vol. 14, no. 2, pp. 89-93, June 2011.

[22] M. Panahi, S. Bhaumik and D. George, "Power-efficient ultra wideband LNAs for the world's largest radio telescope," *Experimental Astronomy*, vol. 38, no. 3, pp. 359-379, December 2014.